Journal of Biomechanics 97 (2019) 109409

Contents lists available at ScienceDirect

Journal of Biomechanics

journal homepage: www.elsevier.com/locate/jbiomech
www.JBiomech.com

Short communication

Assessment of biomechanical properties of the extracellular and pericellular matrix and their interconnection throughout the course of osteoarthritis

Marina Danalache [a,*], Leonhard Felix Jacobi [a,b], Maik Schwitalle [c], Ulf Krister Hofmann [a,d]

[a] Laboratory of Cell Biology, Department of Orthopaedic Surgery, University Hospital of Tübingen, Waldhörnlestraße 22, D-72072 Tübingen, Germany
[b] Medical Faculty of the University of Tübingen, D-72076 Tübingen, Germany
[c] Winghofer Medicum, Röntgenstraße 38, D-72108 Rottenburg am Neckar, Germany
[d] Department of Orthopaedic Surgery, University Hospital of Tübingen, Hoppe-Seyler-Straße 3, D-72076 Tübingen, Germany

ARTICLE INFO

Article history:
Accepted 6 October 2019

Keywords:
Articular cartilage
Osteoarthritis
Atomic force microscopy
Cellular arrangement
Pericellular matrix
Extracellular matrix
Elasticity

ABSTRACT

During osteoarthritis (OA)-triggered cartilage degeneration, the chondrocytes spatially rearrange from single to double strings, and then to small and finally big clusters. Both the extracellular matrix (ECM) and the pericellular matrix (PCM) progressively degrade in osteoarthritis, changing the overall mechanical properties of the cartilage. We investigated the mechanical properties particularly elasticity of the ECM and PCM and their interconnection as a function of chondrocyte spatial organisation.

Human articular cartilage samples from 30 patients were categorised according to their cellular pattern. Elasticity of the ECM and PCM was assessed by means of atomic force microscopy (AFM). Significant decreases were observed in the elasticity of both the ECM and the PCM with each change of cellular pattern, except from single to double strings in the ECM ($p = 0.072$). Spatial reorganisation strongly correlated with the elasticity of the ECM ($r = -0.768$, $p < 0.001$) and of the PCM ($r = -0.729$, $p < 0.001$). The ECM/PCM ratio remained unchanged ($r = -0.099$, $p = 0.281$).

This study is the first to describe and quantify the differences in the elastic moduli of the ECM in relation to the PCM on the basis of chondrocyte spatial arrangement. This study shows that the elastic changes of the ECM and the PCM occur simultaneously, unidirectionally, and to a comparable degree.

1. Introduction

Osteoarthritis (OA) is a highly common degenerative joint disease primarily characterised by irreversible damage of the articular cartilage that leads to strong pain and disability among adults. Within the articular cartilage, the chondrocytes form specific patterns, which appear to be dependent on, and specific for each joint, as well as its loading mechanism (Rolauffs et al., 2008; Schumacher et al., 2002). Whereas in healthy tissue areas, chondrocytes are arranged as single strings, with the onset and progression of OA, cellular rearrangement occurs: double strings arise (Rolauffs et al., 2010), followed by clustering of the cells in late disease stages, represented by the presence of small and then finally large clusters (Lotz et al., 2010).

As in any other connective tissue, the articular cartilage is composed of a vast and dense extracellular matrix (ECM). An additional feature of cartilage is the presence of a thin and highly specialised matrix called the pericellular matrix (PCM), which encompasses the chondrocytes. This PCM is both biochemically and biomechanically distinct from the ECM. Initiation and progression of OA is characterised by elevated production of proteolytic enzymes (e.g. matrix metalloproteinases (MMPs)), which are responsible for the degradation of various PCM and ECM components (Hollander et al., 1995), leading ultimately to cartilage damage and loss. These matrix compositional changes result in altered mechanical environments of the cells within the cartilage matrix (Alexopoulos et al., 2003; Wilusz et al., 2013). Even though several studies have investigated the ECM with respect to the PCM, as well as their subsequent biomechanical properties (Darling et al., 2010; McLeod

Abbreviations: AFM, atomic force microscopy; ECM, extracellular matrix; EM, elasticity modulus; PCM, pericellular matrix; OA, osteoarthritis; MMP, matrix metalloproteinase.

* Corresponding author.
E-mail addresses: marina.danalache@med.uni-tuebingen.de (M. Danalache), m.schwitalle@winghofer-medicum.de (M. Schwitalle), ulf.hofmann@med.uni-tuebingen.de (U.K. Hofmann).

https://doi.org/10.1016/j.jbiomech.2019.109409
0021-9290/

et al., 2013; Wilusz et al., 2012; Wilusz et al., 2013), the reported findings so far are based on macroscopic surface parameters to grade the tissue and thus represent only the micromechanical picture at an averaged level. The aim of this study was to evaluate OA-related elasticity changes in the ECM and the PCM and their relationship to each other in native human articular cartilage on the basis of tissue categorisation by cellular spatial organisation.

2. Materials and methods

2.1. Tissue sample acquisition and tissue preparation

Articular cartilage samples were obtained from patients undergoing total knee arthroplasty at the University Hospital of Tübingen, Department of Orthopaedic Surgery, and the Winghofer Medicum Clinic, Rottenburg a.N. Institutional and ethical approval was obtained before the commencement of the study (project number 672/2016BO2). Preparation of the tissue for AFM measurements was performed as previously described (Danalache et al., 2019). In brief, the topmost layer of articular cartilage was sectioned by using a Leica CM3050S cryotome (Leica Biosystems, Wetzlar, Germany) at a thickness of 35 μm. Tissue slices were fixed onto tissue culture dishes (TPP Techno Plastic Products AG, Trasadingen, Switzerland) covered with Leibovitz's L-15 medium without L-glutamine (Merck KGaA, Darmstadt, Germany) followed by AFM indentation measurements.

2.2. Biomechanical elastic property assessment of the ECM and PCM via AFM

Elastic moduli (EM) of the ECM and PCM were assessed by means of atomic force microscopy (AFM) exactly as previously described by Danalache et al. (Danalache et al., 2019). Briefly, an AFM system (CellHesion 200, JPK Instruments, Berlin, Germany) integrated into an inverted phase contrast microscope (AxioObserver D1, Carl Zeiss Microscopy, Jena, Germany) was used for the measurements. The elastic properties of the ECM and PCM in relation to the different cellular patterns were assessed by performing indentations over the chosen region of interest identified by microscopic examination. Two distinct patterns were measured on each histologic cut, whereby two sites were measured per chosen pattern. To increase accuracy, we performed nine measurement repetitions on each measurement site. Whereas for the PCM measurements, the cantilever was placed in close proximity to the nuclei of the cells, the ECM was measured in close proximity to the PCM region, defined by a region of interest of 100 μm × 100 μm, in which no cells were present (Fig. 1). The Young's modulus was calculated from the force-distance curves by using the Hertz model incorporated into the data processing software (JPK Instruments, Berlin, Germany). AFM measurements for the ECM and PCM were performed on articular cartilage from a total of 30 patients. Thus, a total of 2160 measurements were conducted for each of the two matrices (ECM and PCM). For the final analysis, one value per spatial pattern, type of matrix, and patient was used.

2.3. Statistical analysis

The median of the nine AFM measurements per chosen measurement position was calculated, and, from the two patterns measured per histologic cut, the arithmetic mean of these two calculated medians was used for further analyses. The ECM-PCM interconnection was assessed by calculating the ratio between these two matrices. Experimental results were compared with the Friedman test, Dunn's pairwise test being used for post hoc analysis. The Benjamini-Hochberg false discovery rate correction was used on the basis of alpha = 0.05. The Spearman correlation coefficient was used to evaluate the relationship between the ECM, the PCM, and the ECM/PCM ratios, with the different cellular arrangements. Statistical analysis was performed with SPSS Statistics 22 (IBM Corp., Armonk, NY, USA).

3. Results

In locally uncompromised cartilage depicted by single strings, Young's modulus was 132 (44–472) kPa for the ECM and 65 (28–224) kPa for the PCM, thus showing that elasticity was twice as high for the ECM as it was for the PCM (Table 1). Throughout all changes of spatial cellular organisation, significant decreases could be observed in the EM for both the ECM and the PCM, the only exception being at the transition from single to double strings in the ECM ($p = 0.072$) (Fig. 2, Table 2). The continuous decrease in tissue elasticity led to a much weakened tissue structure in areas with advanced tissue destruction characterised by big clusters, with a Young's modulus of 18 (3–64) kPa for the ECM and only 13 (1–38) kPa for the PCM. A strong correlation was observed between the decrease in Young's modulus for both the ECM ($r = -0.768$, $p < 0.001$) and the PCM ($r = -0.729$, $p < 0.001$) and cellular pattern rearrangement.

Although absolute differences in elasticity between ECM and PCM decreased with advancing tissue destruction (Fig. 3A), interestingly, the ECM/PCM ratio remained almost unchanged (Fig. 3B, Table 1). No relevant association was detected between the ECM/PCM ratio and cellular spatial changes ($r = -0.099$, $p = 0.281$).

4. Discussion

We had previously shown a strong decrease in EM of the PCM with each change in spatial pattern along advancing local tissue degeneration (Danalache et al., 2019). While these findings were based on statistically dependent and independent data, these results were now confirmed with statistically independent samples. In examining the values for the ECM, we observed a strong decrease in stiffness with the changes in chondrocyte patterns. Thus changes in spatial pattern are not just correlated with biomechanical characteristics in the immediate cellular microenvironment, but throughout the entire cartilage.

It is widely accepted that osteoarthritic changes affect the cartilage on all levels and that this leads to disruption of the cartilage matrix. It remained unknown, however, whether this matrix degradation preferentially affects the ECM or the PCM. Despite the strong changes in EM values for both structures during OA no statistically significant changes in the ECM/PCM ration could be observed. This implies that the changes of the ECM and the PCM occur unidirectionally, simultaneously, and to a comparable degree, suggesting that the underlying destructive mechanisms are of the same nature. Interestingly, Wilusz et al. (Wilusz et al., 2013), who also measured and calculated a PCM/ECM ratio, described an increase in the PCM/ECM modulus ratio from 0.36 ± 0.06 in macroscopically normal medial condyle cartilage to 0.56 ± 0.13 in OA cartilage, indicative of a relatively more stable PCM in OA. It must be borne in mind, however, that Wilusz's measurements were not specified according to cellular organisation. Regarding the relative increase in EM of the PCM compared to the ECM in advanced OA, it can be speculated that the structure measured around the cells in advanced OA is actually of a different nature: It had been described, that in advanced local tissue degeneration delineated by the presence of big clusters, the PCM is mostly lost around the cells (Felka et al., 2016); instead, a similar structure of densely packed tissue arises around the lacunae. When

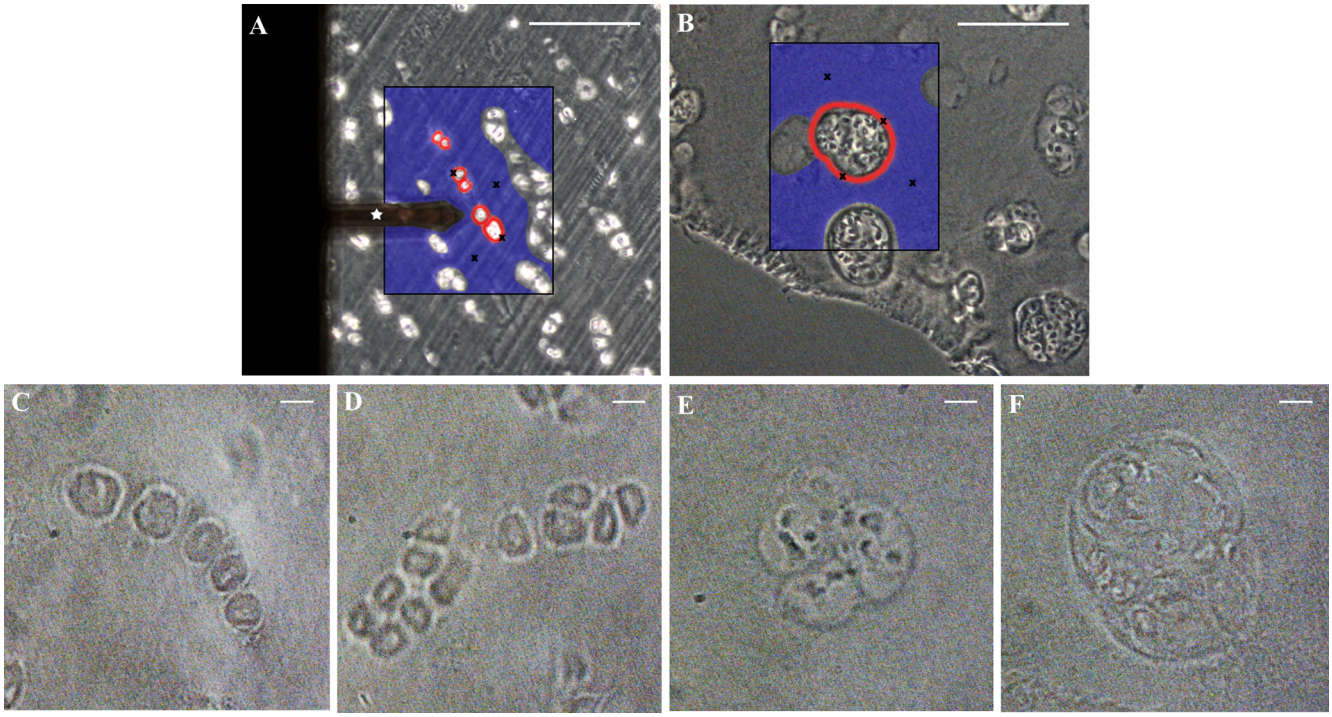

Fig. 1. Representative AFM measurements of the extracellular matrix (ECM) and pericellular matrix (PCM) regions of human articular cartilage. Elastic moduli of the PCM (red zone) and ECM (blue region) (**A/B**) were assessed for various cellular patterns in osteoarthritic cartilage, e.g.: strings (**A/C**), double strings (**D**), small clusters (**B/E**), and big clusters (**F**). The experimenter-selected measurement positions of the ECM and PCM per patient sample are also graphically indicated (black crosses). The cantilever used for the indentations is indicated by a white star. (**A/B**) 10x magnification with scale bar (white) measuring 100 μm; (**C-F**) 40x magnification with scale bar representing 10 μm. (For interpretation of the references to colour in this figure legend, the reader is referred to the web version of this article.)

Table 1
Young's moduli of the ECM and the PCM as assessed by AFM.

Variable	Cellular organisational pattern			
	SS	DS	SC	BC
ECM	132 (44–472)	99 (17–308)	48 (13–106)	18 (3–64)
PCM	65 (28–224)	47 (9–150)	28 (2–70)	13 (1–38)
ECM/PCM ratio	2.0 (0.9–7.5)	2.0 (1.0–5.2)	1.9 (0.9–16.1)	1.7 (1.1–6.4)

Values displayed in kPa and as median (minimum - maximum). Abbreviations: ECM - extracellular matrix, PCM - pericellular matrix, AFM - atomic force microscopy, SS - single strings, DS - double strings, SC - small clusters, BC - big clusters.

the PCM in large clusters is measured, it could be this neo-structure that is measured, thus leading to relatively higher EM in comparison with values from the ECM where no such neo-structure forms.

Because many of the catabolic enzymes such as MMPs are synthesised by the chondrocytes (Aigner et al., 2003; Hembry et al., 2001), it could be hypothesised that the local MMP concentration is higher in the immediate pericellular surrounding (Wilusz et al., 2013). This would be supported by the finding that – if the articular surface is disregarded – within the cartilage, collagen type II and aggrecan degradation epitopes are first observed in the PCM and territorial matrix and only later appear in the ECM (Hollander et al., 1995; Plaas et al., 2007). In contrast, the effect that MMPs seem to have on micromechanical properties on the PCM is comparable to that on the ECM, or they even seem to have less impact on the PCM. This can only be explained by a higher resilience of the PCM to enzymatic digestion (Wilusz and Guilak, 2014), by a higher effort of the chondrocytes to repair the PCM than to repair the ECM, or by an overall higher affinity of the MMPs to collagen type II than to collagen type VI. Interestingly, while ECM EM were significantly reduced after enzymatic digestion of aggrecan, chondroitin/dermatan sulphate, and hyaluronan, the micromechanical properties of the PCM were unaffected by these enzymatic digestions and were significantly reduced by only 24% following elastase digestion (Wilusz and Guilak, 2014). With respect to possible PCM repair, it has been reported that despite local enzymatic degradation of PCM components (Plaas et al., 2007; Polur et al., 2010), enlarged chondrons (i.e. the chondrocytes, including their local PCM) are prevalent in OA cartilage (Lee et al., 2000; Poole et al., 1991). This increase in chondron volume has been speculated to be due to the effects of a net increase in biosynthesis and deposition of PCM macromolecules, especially collagen type VI (Hambach et al., 1998), coupled with a more loosely organised ultrastructure in the pericellular region (Soder et al., 2002).

Interestingly, Darling et al. (Darling et al., 2010) described a constant ratio of PCM to ECM across three different species (human, murine, and porcine), indicating that this well-defined and consistent ratio is an intrinsic characteristic of intact cartilage and possibly necessary for adequate chondrocyte functioning. Given this connection between ECM and PCM stiffness, when an attempt is made to preserve the cartilage by, for example, blocking specific MMPs, it seems highly relevant to preserve both the ECM,

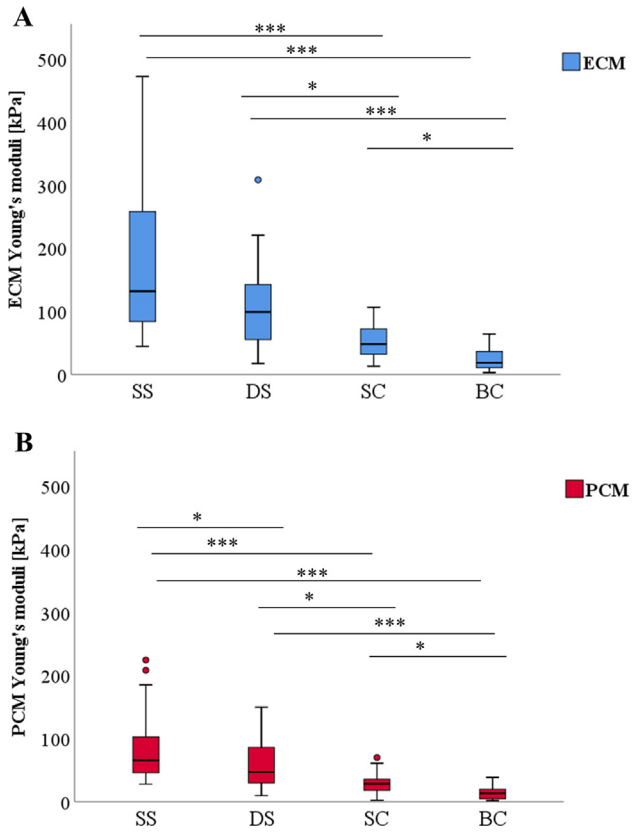

Fig. 2. Comparison of the quantified Young's moduli of the extracellular matrix (ECM) and the pericellular matrix (PCM) as a function of cellular spatial organisation. The boxplots show a constant and continuous decrease of elastic properties for both the ECM (**A**) and the PCM (**B**) with increasingly pathological cellular spatial organisation. *p < 0.05, ***p < 0.001 (exact p values are displayed in Table 2). Abbreviations: SS - single strings, DS - double strings, SC - small clusters, BC- big clusters.

Table 2
Comparison of elasticity measurements of the ECM and the PCM (Young's moduli) as a function of cellular pattern organisation.

Pattern Comparison	ECM	PCM
SS - DS	0.072	0.028
SS - SC	<0.001	<0.001
SS - BC	<0.001	<0.001
DS - SC	0.001	0.002
DS - BC	<0.001	<0.001
SC - BC	0.001	0.006

Significant p-values are marked in bold. Abbreviations: ECM - extracellular matrix, PCM - pericellular matrix, SS - single strings, DS - double strings, SC - small clusters, BC - big clusters.

which is responsible for the macro-mechanical characteristics of the cartilage, and the PCM, which is responsible for chondrocyte resilience and coordinated signalling.

5. Study limitations

Absolute EM values are to be interpreted with care, since they may vary depending on indentation velocity and depth, indenter shape and size, and accurate representation of tip geometry in model fitting (Costa and Yin, 1999; Park et al., 2009; Qian and Zhao, 2018; Stolz et al., 2004) or the thickness of the section. The relationship between the values within one study when using the same parameters should not, however, be affected. A 25 μm

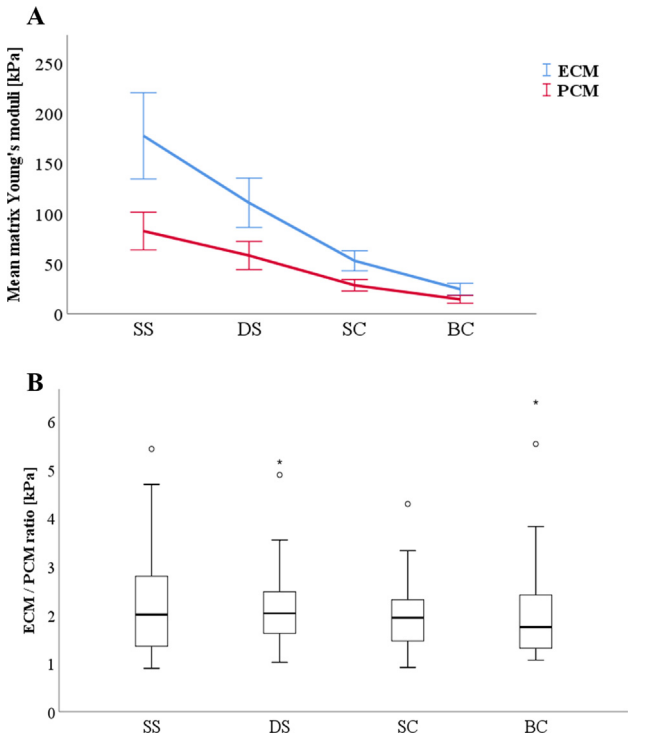

Fig. 3. Relationship of the Young's moduli of the extracellular matrix (ECM) and the pericellular matrix (PCM) as a function of cellular spatial organisation. The more pathological the spatial cellular organisation, the lower Young's modulus values are for both the ECM and the PCM (**A**). Over the course of these spatial cellular changes, no significant change can be observed, however, in the relationship of ECM to PCM elasticity (**B**). Data presented as mean ± standard error (**A**) and boxplots (**B**). Abbreviations: SS - single strings, DS - double strings, SC - small clusters, BC- big cluster.

microsphere attached to the cantilever was employed for AFM indentations. This might have yielded to an average EM determination of the PCM and the encompassed cells, rather than the PCM alone. A smaller microsphere: 2–10 μm might have still provided a higher data resolution and more specific results for the PCM, however to the detriment of the ECM-EM determinations. Moreover OA is a disease that affects the whole joint. It can thus be assumed that in still intact and healthy cartilage, the values for the single strings would have still been higher than those measured in the present study.

6. Conclusion

Our study is the first to describe EM changes of the ECM on the basis of spatial cellular organisation. We showed that, similar to the changes occurring in the PCM, the EM of the ECM are also associated with changes in cellular organisation as a biomarker for local tissue destruction. Moreover, we observed that these changes in the ECM and PCM occur simultaneously, unidirectionally, and to a comparable degree, indicating that events occurring in OA are closely intertwined.

Acknowledgements

We thank the orthopaedic surgeons from the Department of Orthopaedic Surgery of the University Hospital of Tübingen and from Winghofer-Clinic/Rottenburg for providing the tissue samples. We would also like to thank Julius Michael Wolfgart for his help with the graphical representation. We thank Barbara Every, ELS, of BioMedical Editor, for English language editing.

Author contributions

MD designed the study, helped with the statistical analyses, and wrote the manuscript; LFJ performed the experiments, statistical analyses and co-wrote the manuscript; MS provided the cartilage samples, helped interpret the data, and critically revised the manuscript; and UKH designed and supervised the study, helped with the statistical analyses, and wrote the manuscript. All authors read and approved the final manuscript.

Roll of the funding source

No funding was received for the current study.

Declaration of Competing Interest

All authors declare that they have no conflict of interest.

References

Aigner, T., Zien, A., Hanisch, D., Zimmer, R., 2003. Gene expression in chondrocytes assessed with use of microarrays. J. Bone Joint Surg. Am. 85-A Suppl 2, 117–123.
Alexopoulos, L.G., Haider, M.A., Vail, T.P., Guilak, F., 2003. Alterations in the mechanical properties of the human chondrocyte pericellular matrix with osteoarthritis. J. Biomech. Eng. 125, 323–333.
Costa, K.D., Yin, F.C., 1999. Analysis of indentation: implications for measuring mechanical properties with atomic force microscopy. J Biomech Eng 121, 462–471.
Danalache, M., Kleinert, R., Schneider, J., Erler, A.L., Schwitalle, M., Riester, R., Traub, F., Hofmann, U.K., 2019. Changes in stiffness and biochemical composition of the pericellular matrix as a function of spatial chondrocyte organisation in osteoarthritic cartilage. Osteoarthritis Cartilage 27, 823–832.
Darling, E.M., Wilusz, R.E., Bolognesi, M.P., Zauscher, S., Guilak, F., 2010. Spatial mapping of the biomechanical properties of the pericellular matrix of articular cartilage measured in situ via atomic force microscopy. Biophys J 98, 2848–2856.
Felka, T., Rothdiener, M., Bast, S., Uynuk-Ool, T., Zouhair, S., Ochs, B.G., De Zwart, P., Stoeckle, U., Aicher, W.K., Hart, M.L., Shiozawa, T., Grodzinsky, A.J., Schenke-Layland, K., Venkatesan, J.K., Cucchiarini, M., Madry, H., Kurz, B., Rolauffs, B., 2016. Loss of spatial organization and destruction of the pericellular matrix in early osteoarthritis in vivo and in a novel in vitro methodology. Osteoarthritis Cartilage 24, 1200–1209.
Hambach, L., Neureiter, D., Zeiler, G., Kirchner, T., Aigner, T., 1998. Severe disturbance of the distribution and expression of type VI collagen chains in osteoarthritic articular cartilage. Arthritis Rheum 41, 986–996.
Hembry, R.M., Dyce, J., Driesang, I., Hunziker, E.B., Fosang, A.J., Tyler, J.A., Murphy, G., 2001. Immunolocalization of matrix metalloproteinases in partial-thickness defects in pig articular cartilage. A preliminary report. J. Bone Joint Surg. Am. 83, 826–838.
Hollander, A.P., Pidoux, I., Reiner, A., Rorabeck, C., Bourne, R., Poole, A.R., 1995. Damage to type II collagen in aging and osteoarthritis starts at the articular surface, originates around chondrocytes, and extends into the cartilage with progressive degeneration. J. Clin. Investig. 96, 2859–2869.
Lee, G.M., Paul, T.A., Slabaugh, M., Kelley, S.S., 2000. The incidence of enlarged chondrons in normal and osteoarthritic human cartilage and their relative matrix density. Osteoarthritis Cartilage 8, 44–52.
Lotz, M.K., Otsuki, S., Grogan, S.P., Sah, R., Terkeltaub, R., D'Lima, D., 2010. Cartilage cell clusters. Arthritis Rheum 62, 2206–2218.
McLeod, M.A., Wilusz, R.E., Guilak, F., 2013. Depth-dependent anisotropy of the micromechanical properties of the extracellular and pericellular matrices of articular cartilage evaluated via atomic force microscopy. J. Biomech. 46, 586–592.
Park, S., Costa, K.D., Ateshian, G.A., Hong, K.S., 2009. Mechanical properties of bovine articular cartilage under microscale indentation loading from atomic force microscopy. Proc. Inst. Mech. Eng. [H] 223, 339–347.
Plaas, A., Osborn, B., Yoshihara, Y., Bai, Y., Bloom, T., Nelson, F., Mikecz, K., Sandy, J. D., 2007. Aggrecanolysis in human osteoarthritis: confocal localization and biochemical characterization of ADAMTS5-hyaluronan complexes in articular cartilages. Osteoarthritis Cartilage 15, 719–734.
Polur, I., Lee, P.L., Servais, J.M., Xu, L., Li, Y., 2010. Role of HTRA1, a serine protease, in the progression of articular cartilage degeneration. Histol Histopathol 25, 599–608.
Poole, C.A., Matsuoka, A., Schofield, J.R., 1991. Chondrons from articular cartilage. III. Morphologic changes in the cellular microenvironment of chondrons isolated from osteoarthritic cartilage. Arthritis Rheum 34, 22–35.
Qian, L., Zhao, H., 2018. Nanoindentation of Soft Biological Materials. Micromachines, 9.
Rolauffs, B., Williams, J., Grodzinsky, A., E Kuettner, K., A Cole, A., 2008. Distinct horizontal patterns in the spatial organization of superficial zone chondrocytes of human joints.
Rolauffs, B., Williams, J.M., Aurich, M., Grodzinsky, A.J., Kuettner, K.E., Cole, A.A., 2010. Proliferative remodeling of the spatial organization of human superficial chondrocytes distant from focal early osteoarthritis. Arthritis Rheum 62, 489–498.
Schumacher, B.L., Su, J.L., Lindley, K.M., Kuettner, K.E., Cole, A.A., 2002. Horizontally oriented clusters of multiple chondrons in the superficial zone of ankle, but not knee articular cartilage. Anatomical Record 266, 241–248.
Soder, S., Hambach, L., Lissner, R., Kirchner, T., Aigner, T., 2002. Ultrastructural localization of type VI collagen in normal adult and osteoarthritic human articular cartilage. Osteoarthritis Cartilage 10, 464–470.
Stolz, M., Raiteri, R., Daniels, A.U., VanLandingham, M.R., Baschong, W., Aebi, U., 2004. Dynamic elastic modulus of porcine articular cartilage determined at two different levels of tissue organization by indentation-type atomic force microscopy. Biophys. J. 86, 3269–3283.
Wilusz, R.E., DeFrate, L.E., Guilak, F., 2012. Immunofluorescence-guided atomic force microscopy to measure the micromechanical properties of the pericellular matrix of porcine articular cartilage. J. R. Soc. Interface 9, 2997–3007.
Wilusz, R.E., Guilak, F., 2014. High resistance of the mechanical properties of the chondrocyte pericellular matrix to proteoglycan digestion by chondroitinase, aggrecanase, or hyaluronidase. J. Mech. Behav. Biomed. Mater. 38, 183–197.
Wilusz, R.E., Zauscher, S., Guilak, F., 2013. Micromechanical mapping of early osteoarthritic changes in the pericellular matrix of human articular cartilage. Osteoarthritis Cartilage 21, 1895–1903.